

Vibration Isolation of Precision Objects

Eugene I. Rivin, Wayne State University, Detroit, Michigan

The need for vibration isolation of precision and vibration-sensitive objects is increasing continuously. Vibration isolation systems must comply with contradictory specifications, such as requiring reduced stiffness of isolators for better isolation, but higher stiffness for better performance of the object. Recently, expensive active isolation systems have been used to resolve these contradictions. This article shows that a proposed model for vibration isolation of precision objects together with the use of 'smart' constant natural frequency (CNF) isolators substantially widens the application range of inexpensive and reliable passive isolators.

Greater and greater precision and a continuing need to minimize production defects call for improved isolation of sensitive machinery from external vibrations. Vibration isolation systems have to comply with contradictory requirements such as stiffness reduction for better isolation and stiffness increase for better performance of an isolated object.

Ideal vibration isolation of an object should be based on the dynamic characteristics of the object, its sensitivity to vibrations in all six coordinates, and spectral characteristics of vibration excitations from the floor in all six coordinates. These are rarely attainable, especially for typical production sites or R&D establishments where numerous diverse objects, such as precision production and measuring machines and equipment are installed next to vibration producing objects. Some of those that require vibration isolation are themselves vibration exciters (e.g. microlithography steppers and scanners). Such an ideal approach would be useless for real-life situations anyway. Some reasons for this:

1. Vibration levels at installation sites are changing continuously, since they are caused by random factors (loading and speed of passing trucks/trains, random microseismic vibrations, working regimes of production equipment, etc.).
2. Vibration levels are measured before the object and its surrounding equipment are installed. After they are installed (or replaced) the vibration environment may change.
3. Parameters of vibration isolators, even specially designed isolators, have a significant scatter.
4. Unless the object has three mounting points, the weight distribution between isolators is uncertain due to static indeterminacy of the installation. This leads to uncertainty of dynamic characteristics of the isolation system.
5. Many objects have variable weight and weight distribution.
6. Custom isolator designs for each isolated object are unrealistic. Off-the-shelf isolators are available as similar designs, but the stiffness increments between adjacent models range 50-100%. Thus, stiffness values can be realized only within a poor approximation.

All these factors result in suboptimal performance of vibration isolation systems and call for large safety factors to reliably isolate critical objects. This is important both for precision vibration-sensitive objects and for more numerous vibration-producing objects. The "safety factors" are realized by using very soft isolators, which are more expensive, more bulky, and may cause large undesirable swaying of the objects caused by internal or external excitations. These motions can be reduced by the use of massive and expensive inertia blocks that disrupt production line flexibility.

A common solution in many cases is to use active isolators. Their performance comes with a high price – increased direct costs, reduced reliability, dependence on a power supply, and

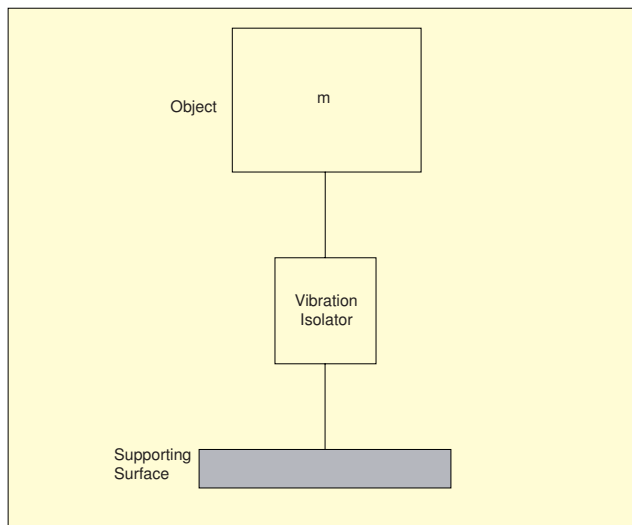


Figure 1. Uni-axial vibration isolation system.

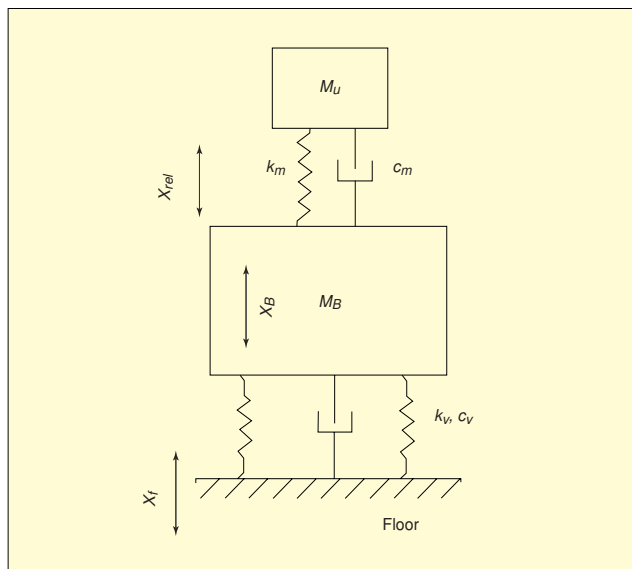


Figure 2. Uni-axial two-mass model of a precision object.

high maintenance especially for systems requiring 3D isolation.

Since active systems are very profitable for isolator providers, passive approaches are often presented as ineffective, low-technology devices. However, passive systems can be significantly improved by: formulating generic isolation requirements for large groups of objects requiring treatment; understanding that natural frequencies (or isolator stiffness values) can be adjusted by judicious use of damping; and by using 'smart' constant natural frequency (CNF) vibration isolators.

First, let's briefly survey principles and criteria of "real-life" vibration isolation systems. There are four basic groups of objects requiring vibration isolation:

- Vibration-sensitive machines and devices (precision machine tools, coordinate measuring machines, or CMMs, electronic devices, etc.). The goal of vibration isolation is to reduce relative vibration amplitudes in the work zone below allowable levels (between tool and workpiece, between components of an electronic device, etc.).
- Vibration-producing machines and devices (metal forming and other impact-generating devices, unbalanced rotors, re-

Based on a keynote presentation at ICSV12, the 12th International Congress on Sound and Vibration, Lisbon, Portugal, July 2005.

reciprocating mechanisms, etc.) The goal of isolation is to reduce the intensity of dynamic excitations transmitted to the supporting structure (floor, foundation, etc.) below permissible levels.

- General-purpose machinery and equipment, neither very sensitive nor very dynamic (e.g., machine tools of normal precision). The goal of isolation is protection from excessive accidental vibrations/shocks from the floor; protection of the environment from occasional intense dynamics within the object (stick-slip vibrations, cutting chatter, turning of non-uniform parts, etc.); reduction of noise and vibration levels; and simplified installation.
- Objects installed on nonrigid structures having high vibration levels (on upper floors of buildings, in vehicles, etc.). The goal is to assure normal functioning of the equipment and to protect very sensitive environments.

Vibration Isolation of Precision Objects

Only the first group (vibration-sensitive objects) is addressed here, but many conclusions and techniques are applicable to other groups. The source of vibration excitation (e.g., the supporting floor for precision objects) and the object to be protected are separated by an auxiliary system comprising vibration isolators or vibration isolating mounts of relatively low stiffness. The mounts weaken dynamic coupling between the source and the object, reducing transmission of unwanted vibration. Figure 1 illustrates the most primitive single-degree-of-freedom isolation system.

Vibration isolation should not impair performance of the object. A surface grinder with a heavy reciprocating table on soft isolators rocks during the table reversal. If the rocking does not fully decay before the new cutting pass starts, the result is a wavy machined surface. This does not occur with stiffer isolators, but protection from floor vibration may become inadequate. Isolation is often used together with other approaches, such as reduction of excitation intensity, changes of mass and stiffness of structural components, dynamic vibration absorbers, etc.

Numerous measurements of floor vibration have demonstrated that maximum vibration amplitudes and their frequency ranges are very consistent for specific types of facilities. A spectrum with constant vibration amplitudes of 3 μm for vertical and 2 μm for horizontal vibration in the 3-20 Hz range would conservatively represent a worst case for manufacturing plant floors. Vertical amplitudes of 0.15 μm and horizontal amplitudes of 0.05 μm in the 3-12 Hz frequency range conservatively represent the worst vibration environment for microelectronic fabricating facilities 'fabs.' Floor vibration amplitudes typically decline quickly in the higher frequency ranges. In many cases, there is no need to measure actual vibration levels if these numbers are used appropriately.

A generalized model of vibration transmission into the work zone of a protected object for each coordinate axis requires at least two degrees of freedom, Figure 2. Floor vibrations with amplitude X_f are transmitted through vibration isolators k_v , c_v to frame/bed of object M_B , holding the 'workpiece.' The generalized 'workpiece' amplitude X_B is then transmitted to the work zone between M_u and M_B , where M_u is the generalized 'toolholder' (relative vibration amplitude X_{relm} where m stands for 'model'). The actual relative vibrations in the work zone are modified by geometric features of the object design that can make the object more or less sensitive to vibration (the design factor γ is different for each coordinate axis),

$$X_{rel} = \gamma X_{relm} \quad (1)$$

Stiffness and damping k_m , c_m represent the object structure. For reasonably designed precision objects, such as precision machine tools, microscopes, etc., the partial natural frequency of the structure described by $M_u - k_m - M_B$ is $f_m \approx 30$ Hz. This is often much higher for precision objects, such as machine tools, and $f_m \approx 10$ Hz for ultra-precision objects such as microlithography tools. The partial natural frequency of the isolation

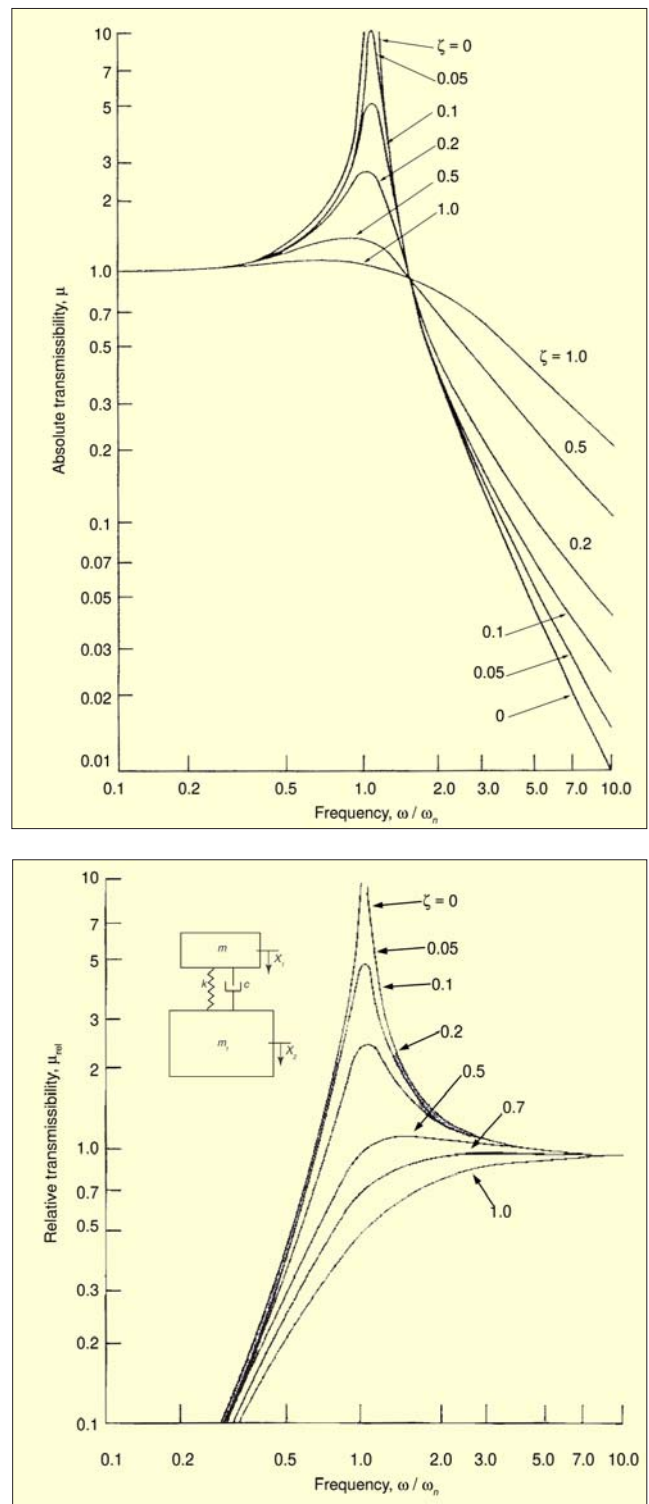


Figure 3. (a) Absolute transmissibility of uni-axial vibration isolation system from floor to object frame; (b) relative transmissibility from object frame to work zone.

system $M_B - k_v$ is usually much lower – $f_v = 10$ -20 Hz for machine tools and $f_v = 1$ -5 Hz for ultra-precision objects. Accordingly, the dynamic isolation system and the dynamic structural system are only weakly dynamically coupled and can be considered independent. Absolute transmissibility μ of the isolation system (from the floor to the bed) is shown in Figure 3a. Relative transmissibility μ_{rel} from the bed to the work zone is shown in Figure 3b.

It is clear from the floor vibration analysis that isolation is required in the above-defined frequency ranges of maximum displacement amplitudes of the floor since the amplitudes diminish quickly at higher frequencies. The majority of precision

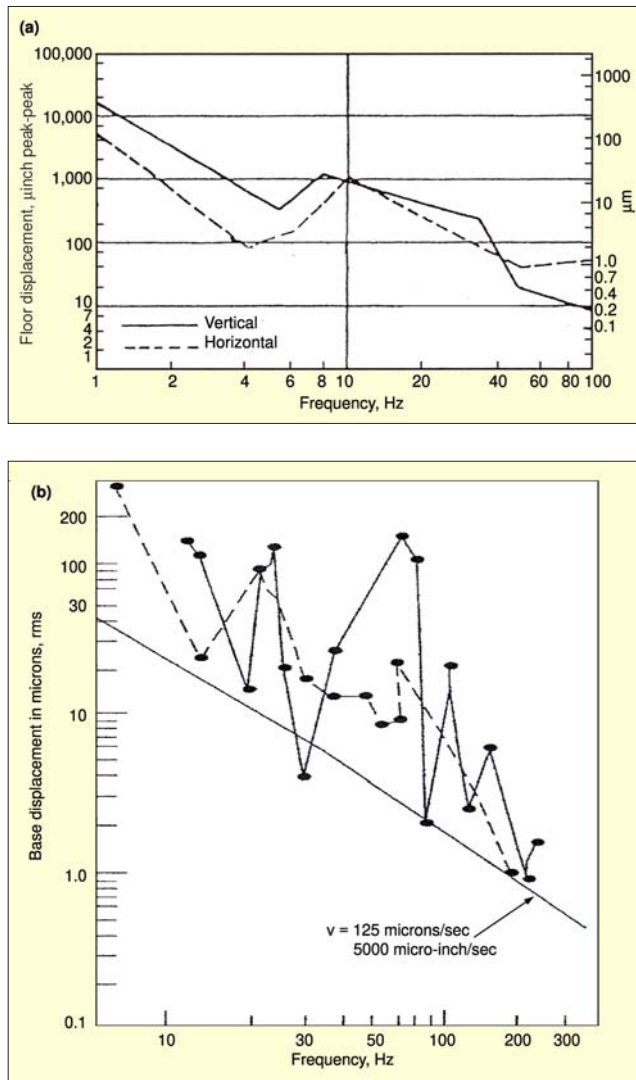


Figure 4. Allowable frame amplitudes for: (a) detectable motion on 1 μm test line for a microlithography stepper; (b) a projection aligner for 0.1 μm image motion.

and ultra-precision objects are much more sensitive to horizontal than to vertical vibrations. For machine tools, the difference is three to 10 times, for ultra-precision objects the difference is from ~ 1.5 times (e.g. for optical microscopes) to about 10 times for microlithography steppers in Figures 4a and 4b.

The above analysis can be summarized by deriving a criterion for vibration isolation of a vibration-sensitive object using the schematic in Figure 5. Figure 5a shows the conservatively generalized floor excitation amplitude X_f (constant amplitude in the appropriate frequency range). Figure 5b shows the vibration displacement amplitude X_B of the object frame vs. frequency resulting from the filtering effect of the vibration isolation system (as in Figure 3a) on the input floor displacement spectrum in Figure 5a. Line 1 corresponds to installation of the object on relatively rigid mounts. Line 2 is for the object on relatively soft isolators having the same damping (resonance amplification) as the rigid mounts (line 1), and line 3 corresponds to installation on isolators having the same stiffness k_v as in case 2, but higher damping.

Figure 5c represents transmissibility from the frame to the relative vibratory displacement in the work zone (as in Figure 3b). Since the vibration isolation system and the structural dynamic system are only weakly coupled and can be considered independent, the transmissibility plot from the floor to the work zone is obtained by multiplying plots in Figures 5b and 5c, resulting in Figure 5d. In Figure 5d, Δ_0 is the allowable amplitude of relative vibration in the work zone specified for a given precision object. For Case 1 (the object on rigid isola-

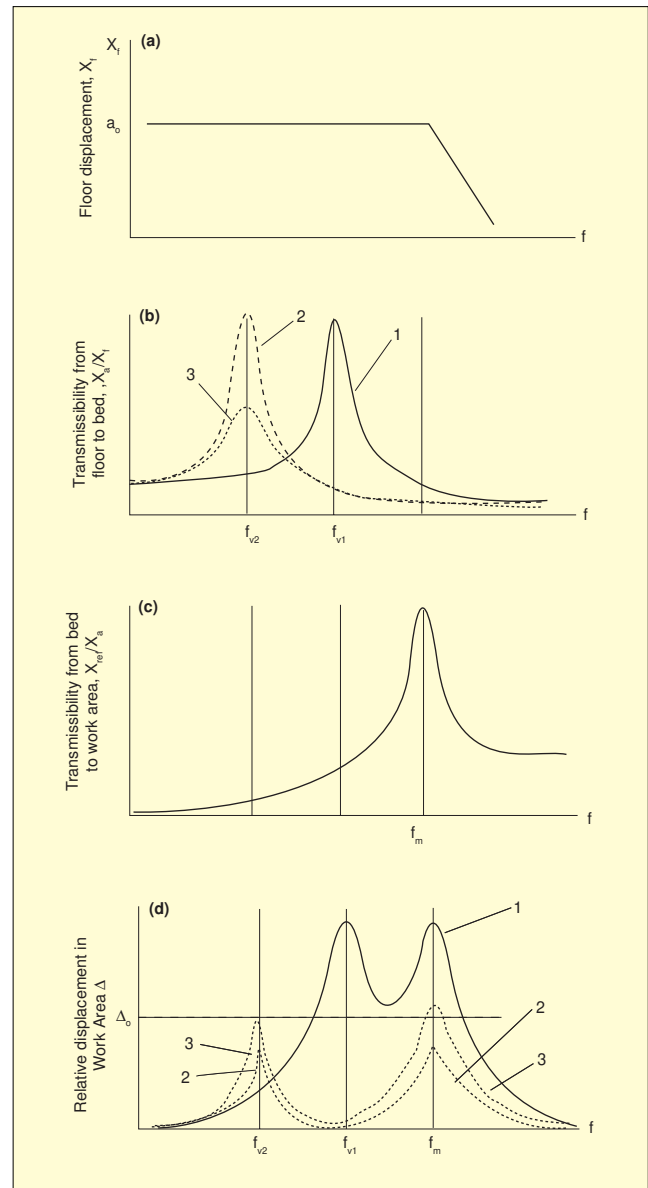


Figure 5. Vibration isolation for broad spectrum floor excitation: (a) floor excitation spectrum; (b) frame vibration spectrum; (c) transmissibility from frame to work zone; (d) spectrum of relative vibration in work zone.

tors), the resulting relative vibrations in the work zone exceed Δ_0 at two resonance frequencies f_{v1} and f_m . For adequately soft isolators (Case 2), both of the resonance peaks in Figure 5d are decreasing below Δ_0 . The first peak is lower because f_{v2} corresponds to the lower sensitivity of the structure $M_B - k_m - M_u$ to the frame vibration. The second peak is lower due to lower transmissibility of the vibration isolation system at the structural natural frequency f_m . Adding damping to the soft isolators without changing their stiffness reduces the first peak (at f_{v2}) even more, while slightly increasing the second peak (at f_m). Figure 5 is drawn with a conservative assumption that f_m is lower than the cut-off frequency of the floor vibration spectrum. Practically, this is not the case, and only the peak at f_{v1} , f_{v2} should be considered. This analysis, validated by thousands of precision object installations, shows that the *vibration isolation systems of precision objects have resonances within their normal working regimes*. Application of a 'textbook' approach to isolation of precision objects from floor vibrations (all floor vibrations must be reduced by 80-90%) would require extremely low (fractions of 1 Hz) natural frequencies f_v . Such systems are extremely bulky, expensive, destabilizing for the isolated objects and, first of all, unnecessary. Unfortunately, such an approach is considered as "politically correct" in vi-

bration isolation applications and is universally used.

If the 80-to-90% reduction of frame vibration as compared with floor vibration is required, the natural frequency f_v of the isolation system should be less than a certain limit, e.g.

$$f_v < f_{v80\%} \quad (2)$$

providing 80% reduction of vibration transmission. Use of analytical expressions for transformations illustrated in Figure 5 results in formulation of the isolation criterion (different for each coordinate axis) for precision objects,

$$\frac{f_v}{\delta_v} = \Phi_v \quad (3)$$

where δ_v is the log decrement of the vibration isolators and Φ_v is the "isolation criterion" guaranteeing that the maximum amplitude in the work zone does not exceed A_0 . Besides resulting in much more practical and economical installations, this approach allows one to modify and improve performance of the isolation system. Isolator stiffness may be increased by increasing damping (e.g., by using high damping material as the isolation element). This also improves resistance to rocking motions due to internal excitations (for example, ultra-precision and vibration-sensitive microlithography tools have heavy stages reciprocating at a high rate of speed).

Reduction of Coupling in Vibration Isolation Systems

It is very important that more intense vertical vibrations of the floor do not excite objectionable horizontal vibrations of the object. This requires analysis of the complete six-degrees-of-freedom vibration isolation system and formulating conditions for decoupling of vertical and two horizontal/rocking modes.

The full set of six equations of motion for a vibration isolation system is quite complex, with motions along all translational and angular coordinate axes dynamically coupled. For a majority of real-life precision objects analyzed in their 'natural' coordinate frames (vertical z , fore-and-aft x and side-to-side y translational axes) the system can be significantly simplified if products of inertia of the object are neglected. Isolators are installed in one horizontal plane (their vertical coordinates $a_z = \text{const}$) with their principal stiffness axes parallel to the x , y , z coordinates – angular stiffness of the isolators is neglected. Then the equations of motion become:

$$\begin{aligned} m\ddot{x}_c + \sum_i k_{x_i} (x_c - x_f) + a_z \sum_i k_{x_i} (\beta - \beta_f) - \sum_i k_{x_i} (\gamma - \gamma_f) &= F_x \\ I_x \ddot{\alpha} - a_z \sum_i k_{y_i} (y_c - y_f) + \sum_i k_{y_i} a_{y_i} (z_c - z_f) + \sum_i (k_{y_i} a_{z_i}^2 + k_{x_i} a_{y_i}^2) \\ (\alpha - \alpha_f) - a_z \sum_i k_{z_i} a_{y_i} (\beta - \beta_f) - a_z \sum_i k_{y_i} a_{x_i} (\gamma - \gamma_f) &= M_x \\ m\ddot{y}_c + \sum_i k_{y_i} (y_c - y_f) - a_z \sum_i k_{y_i} (\alpha - \alpha_f) + \sum_i k_{y_i} a_{x_i} (\gamma - \gamma_f) &= F_y \\ I_y \ddot{\beta} + a_z \sum_i k_{z_i} (x_c - x_f) - \sum_i k_{x_i} a_{x_i} (z_c - z_f) - \sum_i k_{z_i} a_{x_i} a_{y_i} (\alpha - \alpha_f) + \\ \sum_i (k_{x_i} a_{z_i}^2 + k_{x_i} a_{x_i}^2) (\beta - \beta_f) - a_z \sum_i k_{x_i} a_{y_i} (\gamma - \gamma_f) &= M_y \\ m\ddot{z}_c + \sum_i k_{z_i} (z_c - z_f) + \sum_i k_{z_i} a_{y_i} (\alpha - \alpha_f) - a_z \sum_i k_{z_i} a_{y_i} (\beta - \beta_f) &= F_z \\ I_z \ddot{\gamma} - \sum_i k_{x_i} a_{y_i} (x_c - x_f) + \sum_i k_{y_i} a_{x_i} (y_c - y_f) - a_z \sum_i k_{y_i} a_{x_i} (\alpha - \alpha_f) - \\ a_z \sum_i k_{x_i} a_{y_i} (\beta - \beta_f) + \sum_i (k_{x_i} a_{y_i}^2 + k_{y_i} a_{x_i}^2) (\gamma - \gamma_f) &= M_z \end{aligned} \quad (4)$$

Here a_x, a_y, a_z are coordinates of the isolators in the coordinate frame with its origin at the center of gravity (CG) of the object; m, I_x, I_y, I_z – mass and moments of inertia of the object; k_x, k_y, k_z – stiffness constants of the isolators along the coordinate directions; x_c, y_c, z_c – vibratory displacements of the CG; α, β, γ – rotations of the object around axes x, y, z ; $x_f, y_f, z_f, \alpha_f, \beta_f, \gamma_f$ – translational and angular components of the floor motion.

The system of Eq. 4 is still characterized by coupling between all six coordinates. However, if the following conditions are satisfied:

$$\sum_i k_{z_i} a_{x_i} = 0, \sum_i k_{z_i} a_{y_i} = 0 \quad (5)$$

then vertical z vibration of the system is not coupled with motions in other translational or rotational coordinates.

A natural way to comply with Eq. 5 is to find the object weight W distribution between the mounting points and to use isolators whose stiffness constants are proportional to the fraction W_i of the total weight acting on the i th mounting point. Indeed, if each k_{z_i} in Eq. 5 were replaced by W_i , then Eq. 5 becomes an identity, since distances a_x, a_y are measured from the CG. Thus, if vertical stiffness of i th isolator/mount is proportional to W_i ,

$$k_{z_i} = AW_i, A = \text{const.} \quad (6)$$

then Equations 5 are satisfied, since they reflect the moment equilibrium of the object in vertical planes $X-Z$ and $Y-Z$. If also the following conditions are satisfied:

$$\sum_i k_{x_i} a_{y_i} = 0, \sum_i k_{y_i} a_{x_i} = 0 \quad (7)$$

then vibrations both along and about axis Z (coordinates z and γ) are uncoupled. Conditions in Eq. 7 are satisfied if, in addition to Eq. 6, ratios $k_x/k_z, k_y/k_z = \text{const.}$ for all isolators. If also:

$$\sum_i k_{z_i} a_{x_i} a_{y_i} = 0 \quad (8)$$

then the system in Eq. 4 separates into two independent equations corresponding to coordinates z and γ , and two pairs of coupled equations for coordinates $x-\beta$ and $y-\alpha$. Eq. 8 is satisfied if the object has at least one plane of symmetry. A complete decoupling is achieved if Equations 5, 7, and 8 are satisfied, all isolators are located in the same plane as the CG, or

$$a_{z_i} = 0 \quad (9)$$

Eq. 9 can be realized if the object is attached to a massive "inertia block" and then placed on isolators at the new CG level, or if the isolators are supported by brackets at the CG level. This effect can be also achieved with inclined isolators in the $X-Z$ and/or $Y-Z$ planes of the object. Coordinates x and/or y can also be uncoupled if angular stiffness values of isolators in α and/or β directions, neglected in Eq. 4, are made very high. This simply prevents angular vibrations from developing.

Coupling is most important between the vertical and horizontal rocking modes, coordinates z and $x-\beta$ and/or $y-\alpha$. To find the importance of deviations from strict adherence to Eq. 5 for coupling in the vibration isolation system, a typical planar (x, z, β) vibration isolation system in Figure 6a has been studied. The stiffness constants of both elastic mounts in this model are identical, but it represents a general case, since different stiffness values of the isolators can be simulated by shifting the CG position. If the stiffness of each mount is proportional to its weight load, it is equivalent to the central position of CG in the model of Figure 6a.

The system in Figure 6a was simulated for the object with geometric and inertia parameters of a typical production machine excited by a horizontal force acting at the CG level. Figure 6b, 6c, and 6d show amplitude/frequency characteristics of this system at various $a_{x1}/a_{x2} = 1.0-2.5$.

When the symmetry condition $a_{x1} = a_{x2}$ for $k_{z1} = k_{z2}$ (or $k_{z1}a_{x1} = k_{z2}a_{x2}$ for $k_{z1} \neq k_{z2}$) is satisfied, the excitation force acting in the x direction does not excite vibration in the z direction. The rocking ($x-\beta$) vibration has two resonances at frequencies $f_{x\beta}$ and $f_{\beta x}$. When the symmetry condition is not satisfied, the third resonance of the rocking vibration appears at the frequency f_z (vertical natural frequency), and intense vertical vibration of the mass m (caused by the horizontal excitation) develops. Amplitude of this vibration at $k_{z1}a_{x1}/k_{z2}a_{x2} = 1.2$ is $0.35/6.7 \approx 0.05$ of the maximum resonance amplitude of the rocking vibration; at $k_{z1}a_{x1}/k_{z2}a_{x2} = 1.7$ it is $0.95/8 \approx 0.12$ and at $k_{z1}a_{x1}/k_{z2}a_{x2} = 2.5$ it is $1.6/6.5 \approx 0.25$ of the maximum rocking amplitude; it is assumed that $k_{x1}/k_{x2} = k_{z1}/k_{z2} = k_1/k_2$. The results are analogous in cases when the excitation force is vertical or when there

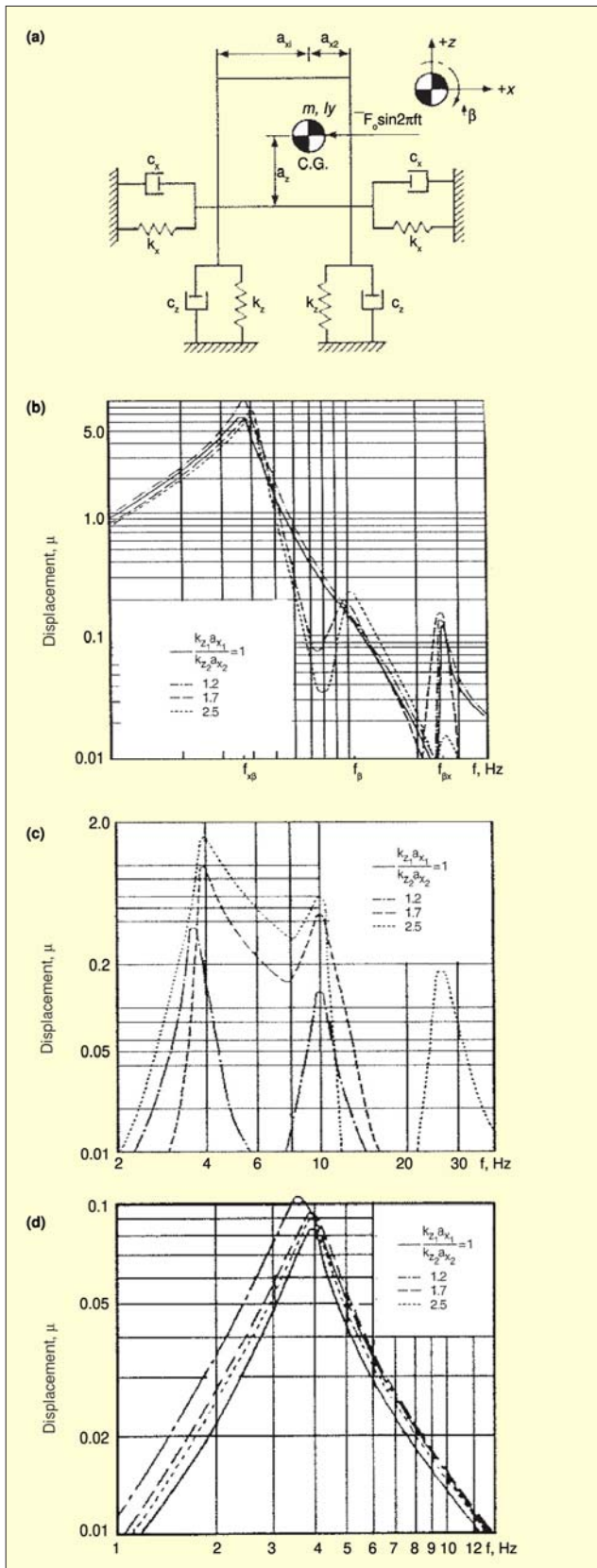


Figure 6. (a) Vibration displacements as a function of frequency for horizontal force excitation through C.G. of planar three-degrees-of-freedom system; (b) z ; (c) x ; (d) β .

is a kinematic excitation from the foundation. For vibration isolation of precision equipment the resonant amplitude of horizontal vibrations of the unit due to a vertical excitation (or vice versa) usually should not exceed ~ 0.2 of the resonant amplitude of vertical vibrations. By interpolation between the above given simulation results, it was concluded that the maxi-

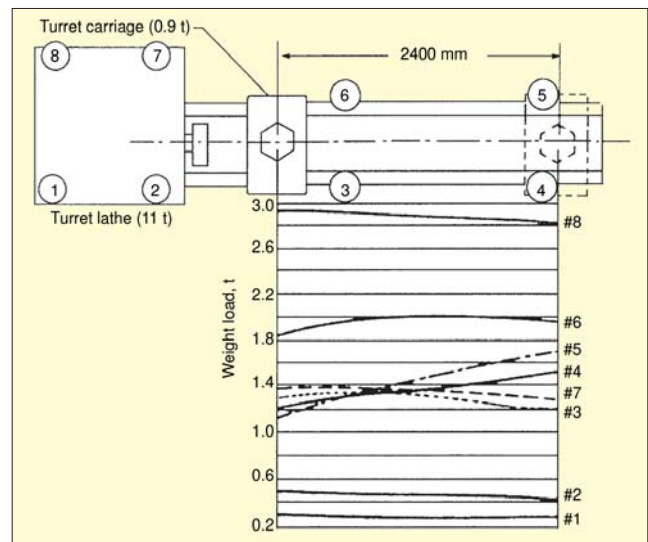


Figure 7. Change of weight distribution on mounts due to tool carriage travel in a turret lathe.

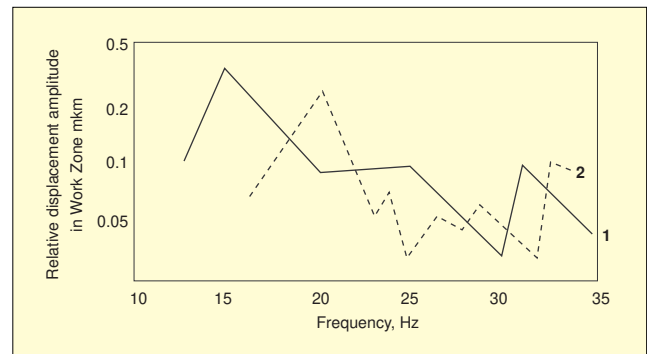


Figure 8. Amplitudes of relative motion between grinding wheel and table of a surface grinder excited by $5 \mu\text{m}$ amplitude floor motion. 1 – rubber-metal CS isolators ($f_z = 15 \text{ Hz}$); 2 – rubber-metal CNF isolators, $f_z = 20 \text{ Hz}$.

mum permissible asymmetry factor should be $k_{z1} a_{x1} / k_{z2} a_{x2} \leq 2.2$.

Correlation of Eq. 6 is critical to satisfy this condition, but it is impossible to achieve with conventional constant stiffness (CS) isolators. Here are some reasons:

1. The total vertical (z -direction) stiffness of all isolators is determined by the desired vertical natural frequency,

$$f_z \approx \frac{1}{2\pi} \sqrt{\frac{\Sigma k_{zi}}{M}} \quad (10)$$

Stiffness of individual isolators should be proportional to the weight loads acting on them. To determine the weight distribution, the CG position must be known. Unless the object has two vertical planes or a vertical axis of symmetry, the CG can be determined either experimentally or by calculation using detailed design drawings.

Experimental determination of the CG is feasible for small/light objects but usually not for heavy machinery. The manufacturers seldom provide this information. Usually, the CG is located from an “expert judgment” by the user, with at least ± 10 – 15% error. For production machinery with heavy moving parts (tables, stages, gantries, etc.) or with widely differing masses of workpieces, the CG can shift significantly. Figure 7 shows the measured weight distribution between the mounting points for a turret lathe, depending on the position of its heavy tool carriage.

2. With the CG position known or assumed, the weight distribution can be uniquely calculated only for a statically determined case when the object is mounted on three supports (isolators). The majority of real-life precision objects are installed on more than three supports. To get the weight distri-

bution in such statically indeterminate cases, additional conditions should be known or assumed.

The weight distribution can change if the mounting surfaces of the object and/or the floor are not flat, or if there are reduced stiffness areas on mounting surfaces, or if the object is not leveled properly. The differences in weight distribution between mounting points before and after leveling of the objects may exceed $\pm 35\%$. Other causes for indeterminacy of the weight distribution are movements of heavy parts in the object (Figure 7) and wide variation of workpiece weights in machine tools and CMMs. Conservatively, deviation of actual weight distribution between the mounting points from calculated estimates can be as much as $\pm 50\%$.

3. After the weight distribution is established, the appropriate isolators compliant with Equations 6 and 10 are selected. Lines of commercial CS vibration isolators have ratios of static stiffness coefficients between adjacent mounts in the line ~ 1.2 – 2.0 , on average ~ 1.6 or ± 1.26 . The accepted tolerance in hardness of rubber is ± 5 durometer units, equivalent to $\pm 17\%$ variation in their stiffness. Often “the adjacent mounts in the line” use different rubber blends, with different dynamic-to-static stiffness ratios K_{dyn} , usually between $K_{dyn} = 1.5$ and 4.0 , an additional ± 1.5 times variation.

Considering all these uncertainties, the stiffness scatter of isolators selected in accordance with the calculated/assumed weight distribution (equivalent to the asymmetry factor) is, conservatively $1.15 \times 1.5 \times 1.26 \times 1.17 \times 1.5 \approx \pm 4$ times. Thus conditions in Eq. 5 are not satisfied even in the first approximation, leading to strong coupling between vertical and horizontal/rocking modes in vibration isolation systems using CS isolators.

Constant Natural Frequency (CNF) Isolators

CNF isolators have their stiffness proportional to the applied weight load, thus the decoupling conditions are automatically satisfied, making a CNF isolator a passive smart element. The stiffness values in all directions of a CNF isolator are proportional to the load in the direction of its main axis (weight load), as expressed by Eq. 6. The deviation of commercially realized CNF isolators from this proportionality does not exceed ± 10 – 15% . They easily satisfy the decoupling condition of Eq. 5 for z direction vibrations and provide a significant coupling reduction for other modes for asymmetrical objects. Even deeper decoupling can be expected for objects having a plane of symmetry.

This statement has been experimentally verified. A precision surface grinder having a plane of symmetry and 20 times more sensitive to horizontal than to vertical floor vibration was tested on CS and on CNF isolators while the floor was vibrating in the z direction with a constant amplitude $5 \mu\text{m}$ in the frequency range of 9–35 Hz. Figure 8 shows amplitudes of relative vibrations between the grinding wheel and the machined surface for installation on five CS isolators with the natural frequency $f_{vz} = 15$ Hz (isolator manufacturer’s recommendation), line 1, and on five CNF isolators, $f_{vz} = 20$ Hz, line 2. The relative vibrations are $\sim 30\%$ lower ($0.25 \mu\text{m}$ vs. $0.35 \mu\text{m}$) when the machine was installed on much (two times) stiffer CNF isolators. We could not find any explanation for this effect other than the dynamic decoupling provided by CNF isolators. With such a decoupling effect, CNF isolators may in some cases replace active and low natural frequency pneumatic isolators.

Designs of CNF isolators. Although various materials are used in isolator designs, the most widely used isolators have rubber flexible elements which use compression deformation for accommodating the weight load. Accordingly, the majority of CNF isolator designs utilize volumetric incompressibility of rubber-like materials, which deform in compression only if they can bulge at the free (unloaded) surfaces.

The first mass-produced CNF vibration isolator for machinery was Russian isolator OB-31, Figure 9. Its flexible element is a monolithic rubber block molded in a relatively simple mold cavity, but its core is composed of two quasi-independent rub-

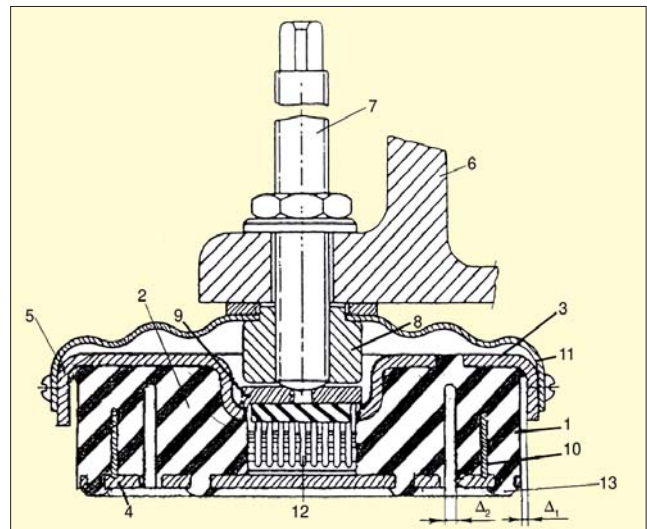


Figure 9. CNF rubber-metal isolator OB-31.

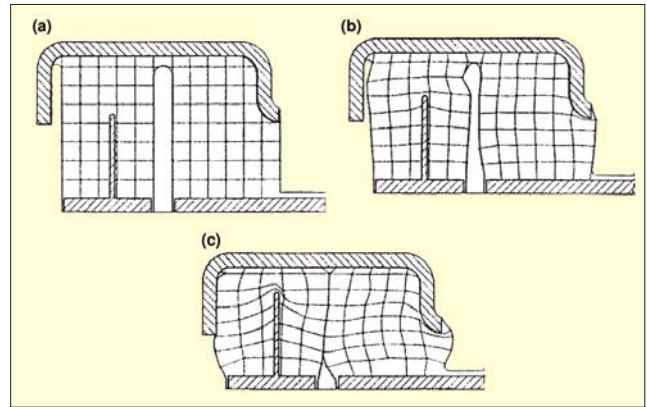


Figure 10. Deformations inside OB-31 isolator; (a) no weight load; (b) low weight load; (c) medium weight load.

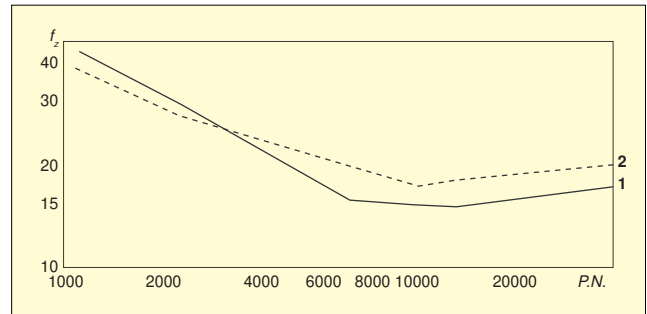


Figure 11. Load-frequency characteristic of OB-31 isolator; 1 – no damper, 2 – with damper.

ber rings 1 and 2. The rings are bonded to top 3 and bottom 4 metal covers. There is a calibrated clearance (gap) Δ_1 between the inner surface of lid 5 and the outer surface of rubber ring 1. Another calibrated gap Δ_2 is between the inner surface of ring 1 and the outer surface of ring 2. At low weight loads, all four side surfaces of rings 1 and 2 are free to bulge, resulting in a relatively low stiffness. With the increasing weight load, the bulge on the outer surface of ring 1 touches lid 5, and the bulge on the inner surface of ring 1 contacts the bulge on the outer surface of ring 2. Thus, the gaps Δ_1 and Δ_2 are gradually filled with the bulging rubber, Figure 10, constraining expansion of the rubber and increasing stiffness. Metal parts 3, 4 can be fabricated with very loose tolerances, since the critical dimensions Δ_1, Δ_2 are defined by the mold. Figure 10 depicts deformation stages of the isolator in Figure 9 obtained by compressing a sector cut from the isolator and placed between transparent plates (with lubrication) maintaining the initial angle of the sector.

Flange 9 has a rubber ‘brush’ 12, immersed in viscous fluid

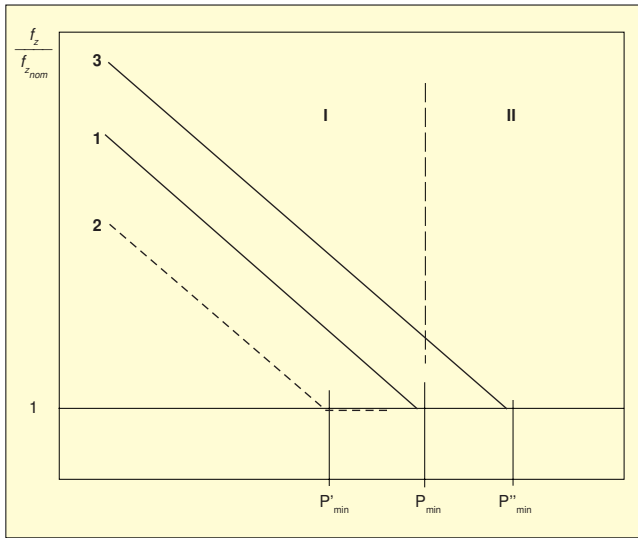


Figure 12. Sensitivity of CS (I) and CNF (II) vibration isolators to production variations.

13, thus generating a three-dimensional damping effect for the isolator. This increases the effective damping of the isolator by 15-20% to $\delta = 0.5-0.7$, thus allowing expansion of the application range of the isolator in accordance with the criterion Φ from Eq. 3. The load-natural frequency f_z characteristic is shown in Figure 11; $f_z = 20 \text{ Hz} \pm 15\%$ within the rated load range from $P_{\min} = 3,200 \text{ N}$ to $P_{\max} = 40,000 \text{ N}$, or $P_{\max}:P_{\min} \approx 13:1$. Since smaller objects usually need vibration isolation with higher natural frequencies, the isolator was successfully used in the load range of 2,000-40,000 N, or effectively with $P_{\max}:P_{\min} \approx 20:1$.

Bottom cover 4 has a thin metal ring 10 welded to it. The ring provides the flexible element with resistance to lateral forces, especially due to compression of the rubber between ring 10 and lid 5 in Figure 9. As a result, the ratio between vertical k_z and horizontal $k_{x,y}$ stiffness is quite constant in the whole load range, $k_z/k_{x,y} = 2.5 \pm 20\%$.

The weight load from object 6 is transmitted by nut 8 to leveling bolt 7, and by washer/flange 9 to top cover 3 and to the rubber block. Spring 11 attaches leveling nut 8 to top cover 3, allowing its vertical displacements during leveling.

Several millions of these isolators have been produced and used for installation of various objects, including numerous vibration-sensitive objects. Although the production line for rubber flexible elements in Russia was not "the best in industry," the natural frequency of the isolators was very consistent, within about $\pm 3\%$. This led to a discovery that CNF isolators have a low sensitivity to production tolerances regardless of design features of their flexible elements (coil springs, rubber flexible elements, etc.), since the rated (nominal) natural frequency of a CNF isolator is determined by its geometry. For small loads on the isolator, $P < P_{\min}$ where P_{\min} is the lower limit of its weight load range, the flexible element usually can be assumed to be linear, Figure 12. The CNF characteristic starts at P_{\min} , at which point deformation of the flexible element is Δ_{\min} . Since at this point the flexible element can still be considered as linear, the natural frequency in the weight load application direction is:

$$f_{z0} \approx \frac{1}{2\pi} \sqrt{\frac{k_z}{m}} = \frac{1}{2\pi} \sqrt{\frac{k_z g}{P_{\min}}} = \frac{1}{2\pi} \sqrt{\frac{g}{\Delta_{\min}}} \quad (11)$$

where k_z is the stiffness of the flexible element on the linear (constant stiffness) segment of its load-deflection characteristic. When the weight load is increasing within the CNF load range $P_{\min}-P_{\max}$, the natural frequency is constant and equal to:

$$f_{z\text{nom}} \approx f_{z0} \quad (12)$$

The nominal natural frequency associated with the CNF isola-

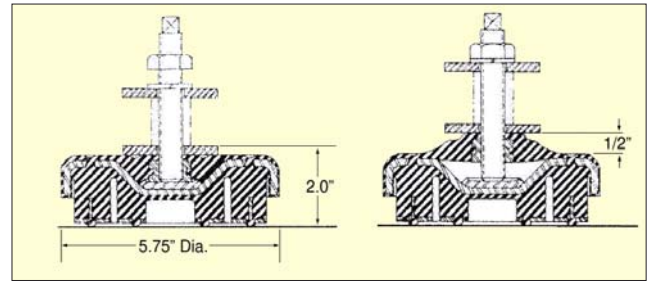


Figure 13. CNF isolator OB-32 before and after leveling.

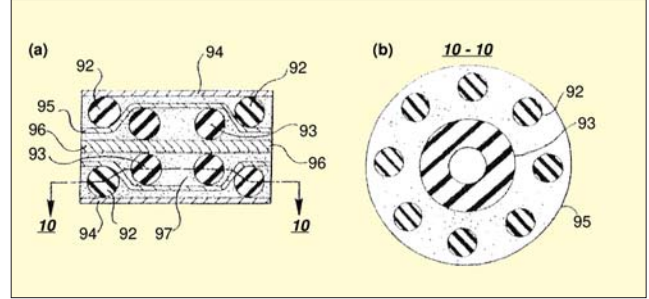


Figure 14. Packaging of streamlined rubber elements by foam matrix without bonding.

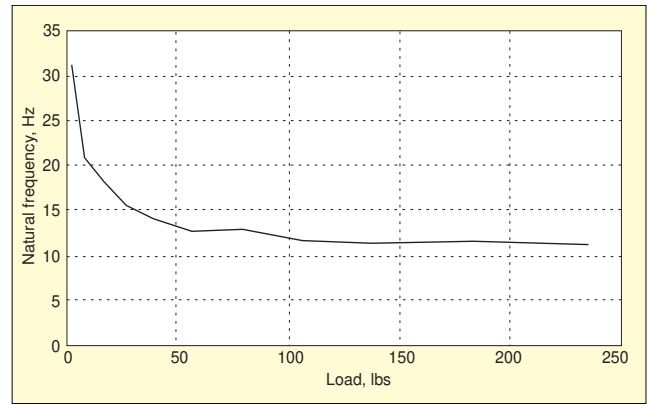


Figure 15. Natural frequency vs. axial compressive load for rubber torus (rubber durometer $H = 30$, median diameter of the torus $D = 50.8 \text{ mm}$, cross-sectional diameter $d = 12.7 \text{ mm}$).

tor is determined by deformation Δ_{\min} of the flexible element at which the load-deflection characteristic becomes a nonlinear CNF characteristic.

For the CNF isolator manufactured without any deviation from the nominal design dimensions, the load-natural frequency characteristic is presented by line 1 in Figure 12. At low weight loads, the isolator has constant stiffness (no touching between the rubber rings 1 and 2 in Figure 9), and its natural frequency f_z decreases with increasing load. As the compression deformation reaches Δ_{\min} (at the load P_{\min} , when the rings start touching), the CNF region begins. If the rubber is softer than specified, the linear region is represented by line 2 indicating lower values of f_z for the same load than for the linear region of line 1. The deformation Δ_{\min} occurs at a lower weight load P'_{\min} ; the CNF characteristic thus begins at a lower load but at the same Δ_{\min} and $f_{z0} = f_{z\text{nom}}$ determined by the value of Δ_{\min} . Similarly, for a harder rubber, the linear region represented by line 3 would indicate higher f_z values than line 1, and the CNF characteristic would begin at a higher weight load but again at the same Δ_{\min} and $f_{z0} = f_{z\text{nom}}$ determined by the value of Δ_{\min} . Thus, the natural frequency remains the same, while the weight load range shifts. This is not significant for most applications, since the load range is usually very broad. This conclusion about robustness of the natural frequency values provided by CNF vibration isolators was validated by monitoring mass-produced ($\sim 700,000$ units a year) vibration isolators in Figure 9 for two years of production.

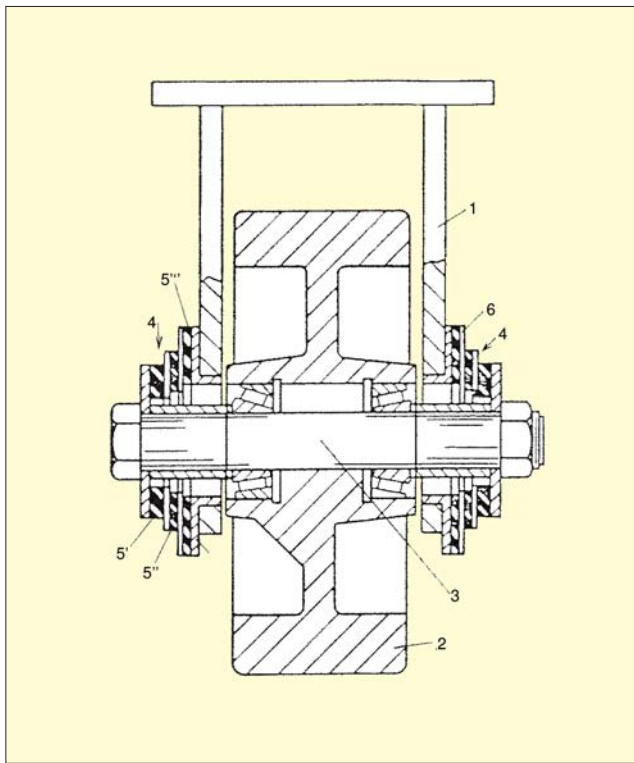


Figure 16. Wheel caster with CNF shear-disc suspension.

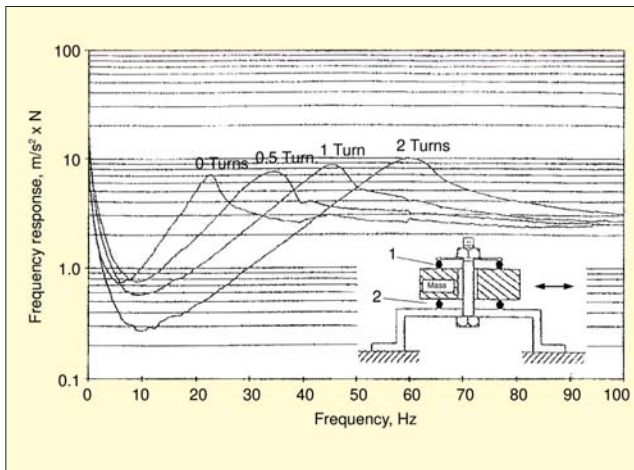


Figure 17. Variable-stiffness device using two CNF isolators.

Variation of the natural frequency did not exceed $\pm 3\%$, while variation of the rubber durometer was observed within ± 7 units (stiffness variation $\pm 25\%$). Dimensional variations of the isolator would, of course, result in variations of f_{znom} , but the dimensions are determined by the mold and usually are quite consistent.

A later modification of the isolator in Figure 9 is shown in Figure 13, where the connection between the leveling nut and the top cover is provided by the rubber membrane. This isolator is easier to produce and has a better appearance. Due to use of a different rubber blend, the damper is not used.

The next generation of CNF vibration isolators based on this design concept was a line of CNF isolators providing for four f_{znom} in broad load ranges and having a smaller $D = 100$ mm instead of $D = 140$ mm for OB-31. Isolators for nominal natural frequencies $f_{znom} = 10, 15, 20$, and 30 Hz had the same metal parts but different Δ_1 and Δ_2 , rubber blends, and height of the rubber element. They covered a range of natural frequencies with $P_{max}:P_{min} = 6-20:1$.

Our extensive research of performance characteristics of streamlined rubber flexible elements led to simplified designs of CNF isolators. Spheres, ellipsoids, toruses, and radially

Commercial Source for CNF Isolators

The CNF isolator in Figures 9 and 13 (U.S. Patent 3,442,475) were developed in the former USSR in the 1960s. It quickly became very popular for all kinds of machinery, from vibration-sensitive precision machine tools and impact producing stamping presses to meat cutters. The biggest users were military-industrial facilities for several reasons. Military production plants were frequently changing both designs and manufacturing processes for their products, requiring quick relocation of the production equipment, not possible with machines grouted to the floor. Also, the military-industrial complex was using the best production equipment having state-of-the-art precision. Yet another reason was a wide use of multistory production buildings (by some estimates, 20 to 25% of newly built manufacturing plants were located in multistory buildings). Obviously, floor vibration levels in such buildings are much higher than in single-story buildings. Still, OB-31 isolators often were able to provide the necessary vibration protection. The author was witnessing a successful installation of precision grinders and jig borers on the 10th floor of a 25-story high rise building using OB-31 isolators. In cases when the isolation was inadequate, OB-31 isolators were used in stacks of two each, thus resulting in a vertical natural frequency of 15 Hz instead of 20 Hz, but still retaining their CNF characteristics.

Users quickly observed good performance results, while using identical isolators for both light and heavy machinery with no need for any calculations. As a result, the production rate for these isolators was 700,000 per year for over 15 years. Currently, three similarly designed vibration isolators (Figure 13) with external diameters of 100 mm and 146 mm with an overall load range of 400-8,000 lbs are available from Advanced Antivibration Components (Div. of Designatronics, Inc., www.vibrationmounts.com).

Many prototypes of CNF pads/mats and mounts per U.S. Patent 5,934,653 using rubber cords and other streamlined rubber elements have been fabricated and successfully tested. These CNF isolators are easy to tailor to specific needs of equipment manufacturers and users.

loaded cylinders are naturally nonlinear in compression, and their nonlinear load-deflection characteristics result in quasi-CNF load-natural frequency characteristics. Stresses under load are very uniform and are two to three times lower for the same compression loads/deformations than for rubber elements bonded to metal plates, thus allowing larger compression deformations. This results in smaller sizes, lower creep rates, and better fatigue resistance. Production of such elements requires relatively simple molds. By changing dimensions/shapes and rubber blends, practically any natural frequency and/or load rating can easily be realized. These elements must not be bonded to metal components, since bonding requires cutouts and other shape distortions resulting in stress risers and reducing the advantages of the ideal shape elements. The specified packaging of rubber and rigid (metal) components of the isolator without bonding can be achieved by using a foam matrix, Figure 14.

Figure 15 shows the load-natural frequency characteristic of a rubber torus in a foam matrix (outer diameter $D = 51$ mm, cross sectional diameter $d = 12.7$ mm) made from $H = 30$ durometer rubber. The nominal natural frequency $f_{znom} = 12$ Hz $\pm 5\%$ is maintained in the load range of 50-240 lbs, $P_{max}:P_{min} = \sim 5:1$. Similar characteristics have rubber flexible elements shaped as spheres. For very soft rubber, the measured values of natural frequency are $f_z = 7.5-8$ Hz for $D = 37.5$ mm; ~ 6.3 Hz for $D = 51$ mm; ~ 5.5 Hz for $D = 64$ mm.

Stiffness ratios $k_z/k_{x,y}$ for ideal shape rubber elements are in

the range of $\eta_{x,y} = 5-9$. These values can be reduced if the lateral deformation of the elements is restrained by rigid inserts embedded in the foam.

A different design of CNF vibration isolator is used for suspension of caster wheels for small vehicles (e.g., in-plant trailers), Figure 16. Axle 3 of wheel 2 is connected to caster 1 via two “shear discs” 4. Each shear disc 4 consists of two-three rubber layers 5 sandwiched between metal discs 6. The holes and outer diameters of metal discs 6 and respective rubber layers 5 are progressively smaller towards the ends of axle 3. The inner surfaces of holes in metal discs 6 will successively land on the axle surface as the shear deformation of rubber layers 5 increases with the increasing weight load. Gradually, shear deformation of the outer layers, 5' then 5'', etc., stops and the stiffness of the suspension increases (hardening nonlinear characteristic). Layers 5 are designed in accordance with the desired payload range and dynamic characteristics of the suspended vehicle. If the load is excessive, bushings 7 land on axle 3 thus preventing excessive shear deformation of the shear discs. This feature is important for in-plant trailers which can be used in a storage mode with supported weight much greater than the maximum payload.

For an empty trailer (1100 N per caster) $f_{z1} = 8.5$ Hz; for a fully loaded trailer (3400 N per caster) $f_{z2} = 7.2$ Hz; for a heavily loaded trailer (6800 N per caster) $f_{z3} = 9.3$ Hz. This CNF characteristic resulted in more than a decimal order of magnitude reduction of dynamic loads on the wheels and on the trailer structure, and in a 16-18 dBA noise reduction (without suspension, noise can reach 110 dBA). The highest noise levels were observed from a moving empty trailer, thus justifying the relatively low f_{z1} . If a linear suspension were used, with $f_z = 8.5$ Hz for the empty trailer it would exhibit $f_z \approx 3.5$ Hz for the heavily loaded trailer, with static deformation over 20 mm. Such low f_z would not lead to further dynamic loads/noise reduction, but would complicate connecting (hitching) of dif-

ferently loaded trailers in a train. With a 10-fold reduction of failures of the axle bearings and wheel treads, the intended noise abatement has also become a money-saving project.

If two CNF isolators are assembled as shown in Figure 17, the load along the z-axis can be adjusted by preloading the bolt independent of the weight load. Effective stiffness of this assembly is varied by adjusting the preload force applied to isolators 1 and 2. Variation of the natural frequency f_x from 20 Hz to 60 Hz was observed with the changing preload (turning the nut), equivalent to ~9:1 stiffness ratio. Such variable stiffness isolators are useful for experimental optimization of vibration isolation systems with complex excitations, with compliant supporting surfaces, as well as for adaptive and other actively controlled isolation systems and dynamic vibration absorbers.

Conclusions

1. The proposed model of vibration isolation of precision objects leads to improved performance while using stiffer isolators with higher damping.
2. In many cases, expensive active isolation systems can be replaced with inexpensive ‘smart’ passive systems.
3. Use of ‘smart’ CNF isolators results in many performance, application, and cost advantages since: they have low sensitivity to production uncertainties; weight-distribution calculations are not required and identical isolators are used under all mounting points; and smaller nomenclature and size of CNF isolators results in lower production costs.
4. CNF isolators can be used as variable stiffness isolators.
5. CNF isolators are natural ‘snubbers’ due to progressively increasing stiffness.

Bibliography

E. I. Rivin, *Passive Vibration Isolation*, ASME Press, 2003.



The author may be contacted at: rivin@eng.wayne.edu.